Well-posedness of nonlocal macroscopic models of multi-population pedestrian flows for domain shape optimization

Paola Goatin, Elena Rossi

Well-posedness of nonlocal macroscopic models of multi-population pedestrian flows for domain shape optimization

Paola Goatin*
Elena Rossi†

October 3, 2024

Abstract

We consider a class of multi-population pedestrian models consisting in a system of nonlocal conservation laws coupled in the nonlocal components and describing several groups of pedestrians moving towards their respective targets while trying to avoid each other and the obstacles limiting the walking domain. Specifically, the nonlocal operators account for interactions occurring at the microscopic level as a reaction to the presence of other individuals or obstacles along the preferred path. In particular, the presence of obstacles is implemented in the nonlocal terms of the equations and not as classical boundary conditions. This allows to rewrite domain shape optimization problems as PDE-constrained problems.

In this paper, we investigate the well-posedness of such optimization problems by proving the stability of solutions with respect to the positions and shapes of the obstacles. A differentiability result in the linear case is also provided. These properties are illustrated with a numerical example.

Key words: Nonlocal systems of conservation laws; multi-population macroscopic pedestrian flow models; domain shape optimization.

1 Introduction

Macroscopic models of pedestrian flows have been developed in the last two decades by the engineering and applied mathematical communities to describe and manage crowd movements, looking at the spatio-temporal evolution of averaged quantities such as density and mean velocity. Hughes [23] sees the crowd as a "thinking fluid" where each individual aims at minimizing its own travel time. Other macroscopic models are based on gas dynamics equations [3, 25], gradient flow methods [30], nonlinear conservation laws with non-classical shocks [10] and time evolving measures [31]. More recently, nonlocal models [7, 9, 12, 15, 18], which account at the macroscopic level for interactions at the microscopic scale, have received a lot of attentions for their mathematical properties and the ability to reproduce self-organised structures, such as lane formation at intersections of groups moving in different directions. These models are based on the assumption that pedestrians follow they preferred velocity field, but they correct the direction of their movement to avoid crowded locations within their (limited) vision cone, see also [22] for a derivation based on the social forces microscopic model [21].

Recently, [5, 17, 18] proposed a novel approach to account for the presence of obstacles in the walking domain in this nonlocal setting: instead of artificially adding a discomfort vector field to keep the density away from boundaries [2, 9, 11, 12], obstacles can be incorporated in the nonlocal operator as high density regions, thus avoiding including them in the preferred velocity

*Université Côte d'Azur, Inria, CNRS, LJAD, 2004 route des Lucioles - BP 93, 06902 Sophia Antipolis Cedex, France, E-mail: paola.goatin@inria.fr

†Università di Modena e Reggio Emilia, Dipartimento di Scienze e Metodi dell'Ingegneria, Via Amendola 2 - Pad. Morselli, 42122 Reggio Emilia, Italy, E-mail: elerossi@unimore.it

field. Remarkably, with this approach, the shape optimization of the walking domain boils down to a classical PDE-constrained optimization problem, and its numerical resolution is very efficient because it does not require any mesh and velocity field recomputing [17]. We recall that the use of obstacles to improve the pedestrian flow and minimize the evacuation time in walking facilities is known to be effective and have been the object of several investigations, see e.g. [16, 20, 24, 29, 33].

Analytically, nonlocal pedestrian models belong to the class of nonlocal systems of conservation laws coupled through the integral terms, which were studied in [1, 9, 13]. In particular, [13] provided a well-posedness result with respect to the Wasserstein distance of order one in the case of measure solutions of linear transport equations. Still for linear systems, [8, 9] studied the differentiability of weak entropy solutions with respect to the initial conditions, showing that the Gateâux derivatives are the Kružkov solutions of the corresponding sensitivity equation.

In this work, we consider a class of nonlocal crowd dynamics models for $N \geq 1$ populations characterized by their destinations and/or speed laws, and trying to avoid each other in a delimited environment. Namely, we focus on the following initial-boundary value problem for a nonlocal system of N conservation laws that describes the evolution of the pedestrian densities $\boldsymbol{\rho} = (\rho^1, \dots, \rho^N)^T$ as a function of time t and position $\mathbf{x} = (x_1, x_2)$ on a walking domain $\Omega \subset \mathbb{R}^2$:

$$\begin{cases} \partial_t \rho^k + \operatorname{div}_{\mathbf{x}} \left[f_k \left(\rho^k \right) \boldsymbol{\nu}^k \left(t, \mathbf{x}, \mathcal{J}^k[\boldsymbol{\rho}] \right) \right] = 0, & \mathbf{x} \in \Omega, t \geq 0,\ k = 1, \dots, N, \\ \boldsymbol{\rho}(0, \mathbf{x}) = \boldsymbol{\rho}_0(\mathbf{x}), & \mathbf{x} \in \Omega, \\ \boldsymbol{\rho}(t, \mathbf{x}) = 0, & \mathbf{x} \in \partial\Omega, t \geq 0. \end{cases} \tag{1}$$

Here, $\boldsymbol{\nu}^k = (\nu_1^k, \nu_2^k)$, $k = 1, \dots, N$, are vector fields describing the direction of movement of the k-th population, $\mathcal{J}^k$ is a nonlocal operator, i.e. $\mathcal{J}^k[\boldsymbol{\rho}] = \left(\mathcal{J}^k[\boldsymbol{\rho}(t)] \right)(\mathbf{x})$, and $\boldsymbol{\rho}_0$ is a given initial datum. Usually, the vector fields $\boldsymbol{\nu}^k$ consists of a fixed smooth vector field of preferred directions (e.g. given by the regularized solution of an eikonal equation) together with nonlocal correction terms depending on the current density distribution.

To account for the presence of boundaries, in the form of walls or other obstacles, we assume that $\Omega^c = \mathbb{R}^2 \setminus \Omega$ is a compact set consisting of a finite number $M \in \mathbb{N}$ of connected components $\Omega^c = \Omega_1^c \cup \ldots \cup \Omega_M^c$. Similarly to [5], we consider that the nonlocal operators are evaluated on the augmented density $\boldsymbol{\rho}_\Omega : \mathbb{R}^2 \to \mathbb{R}_+^{N+1}$ accounting for the presence of obstacles and defined as follows:

$$\rho_\Omega^k := \begin{cases} \rho^k & \text{if } k = 1, \dots, N, \\ \sum_{\ell=1}^M R_{N+\ell} \chi_{\Omega_\ell^c} & \text{if } k = N+1, \end{cases} \tag{2}$$

with $R_{N+\ell} > 0$, $\ell = 1, \dots, M$, big enough so that $\boldsymbol{\nu}^k \left(t, \mathbf{x}, \mathcal{J}^k[\boldsymbol{\rho}_\Omega] \right) \cdot \mathbf{n}(\mathbf{x}) \leq 0$ for all $\mathbf{x} \in \partial\Omega$, $t \geq 0$, $\mathbf{n}$ being the outward normal to Ω. In this way, the domain Ω is invariant and (1) is equivalent to the Cauchy problem

$$\begin{cases} \partial_t \rho^k + \operatorname{div}_{\mathbf{x}} \left[f_k \left(\rho^k \right) \boldsymbol{\nu}^k \left(t, \mathbf{x}, \mathcal{J}^k[\boldsymbol{\rho}_\Omega] \right) \right] = 0, & \mathbf{x} \in \mathbb{R}^2, t \geq 0,\ k = 1, \dots, N, \\ \boldsymbol{\rho}(0, \mathbf{x}) = \boldsymbol{\rho}_0(\mathbf{x}), & \mathbf{x} \in \mathbb{R}^2, \end{cases}$$

where we have set $\rho_0^k(\mathbf{x}) = 0$ for $\mathbf{x} \in \Omega^c$, $k = 1, \dots, N$.

Aiming at guaranteeing the well-posedness of the above mentioned optimization problems, we are interested in proving the stability of solutions with respect to the shape of the domain, i.e. the positions and shape of obstacles Ω_ℓ^c, $\ell = 1, \dots, M$, see Section 2. Moreover, in Section 3 we show

that a differentiability result with respect to the shape of the domain Ω holds in the linear case. A numerical study of a shape optimization problem is finally presented in Section 4, while conclusions and perspectives are discussed in Section 5.

2 Analytical results

We set $\mathbb{R}_+ = [0, +\infty[$. We denote by I the time interval $\mathbb{R}_+$ or $[0, T]$, for a fixed $T > 0$. We set also $\Sigma_t = [0, t] \times \mathbb{R}^2 \times \mathbb{R}^m$ for $t \in \mathbb{R}_+$. Throughout, the number of equations N, the number of connected components of Ω^c, the integer m and the strictly positive constants R_k, $k = 1, \dots, N + M$, are fixed, with $N, M, m \geq 1$.

We assume the following:

(**Ω.1**) The domain $\Omega \subseteq \mathbb{R}^2$ is a non-empty open set with smooth boundary $\partial\Omega$, so that the outward normal $\mathbf{n}(\mathbf{x})$ is uniquely defined for all $\mathbf{x} \in \partial\Omega$. Moreover, we assume that $\Omega^c = \mathbb{R}^2 \setminus \Omega$ is a compact set consisting of a finite number M of connected components.

(**Ω.2**) For all $k = 1, \dots, N$, the vector fields $\boldsymbol{\nu}^k$ point inward along the boundary $\partial\Omega$ of Ω, i.e. $\boldsymbol{\nu}^k \left(t, \mathbf{x}, \mathcal{J}^k[\boldsymbol{\rho}_\Omega]\right) \cdot \mathbf{n}(\mathbf{x}) \leq 0$ for all $\mathbf{x} \in \partial\Omega$, $t \geq 0$.

($\boldsymbol{f}$) $f_k \in \left(\mathbf{C^2} \cap \mathbf{W^{2,\infty}}\right)(\mathbb{R}_+; \mathbb{R}_+)$ with $f_k(0) = f_k(R_k) = 0$ for all $k = 1, \dots, N$.

Assumption (**Ω.2**) guarantees the invariance of the domain Ω, i.e. if $\operatorname{supp} \rho^k(0, \cdot) \subset \Omega$, then we have that $\operatorname{supp} \rho^k(t, \cdot) \subset \Omega$ for all $t > 0$, so that the boundary condition become useless and the problem can be studied on the whole plane $\mathbb{R}^2$. In particular, when considering functional norms of ρ^k on $\mathbb{R}^2$, we have $\rho^k(t, \mathbf{x}) = 0$ for $\mathbf{x} \in \Omega^c$.
Besides, assumption ($\boldsymbol{f}$) provides a maximum principle, guaranteeing that each component ρ^k of the solutions stays positive and bounded below R_k, if the initial data do. We remark that the nonlinearities introduced by the functions f_k prevent the application of results based on Lagrangian solutions and not requiring entropy conditions, such as [9, 13, 27]. In particular, in Section 3 we have to set $f_k = \mathrm{Id}$ for all $k = 1, \dots, N$, to provide differentiability, thus violating ($\boldsymbol{f}$), see Remark 1.

We now need to introduce some notation and further assumptions.
For $k = 1, \dots, N$, given the map $\boldsymbol{\nu}^k \colon I \times \mathbb{R}^2 \times \mathbb{R}^m \to \mathbb{R}^2$, where $(t, \mathbf{x}, A) \in I \times \mathbb{R}^2 \times \mathbb{R}^m$, we set

$$
\begin{aligned}
\nabla_{\mathbf{x}} \boldsymbol{\nu}^k(t, \mathbf{x}, A) &= \left[\partial_{x_j} \nu_i^k(t, \mathbf{x}, A)\right]_{\substack{i=1,2 \\ j=1,2}} \in \mathbb{R}^{2\times 2}, \\
\nabla_A \boldsymbol{\nu}^k(t, \mathbf{x}, A) &= \left[\partial_{A_j} \nu_i^k(t, \mathbf{x}, A)\right]_{\substack{i=1,2 \\ j=1,\dots,m}} \in \mathbb{R}^{2\times m}, \\
\nabla_{\mathbf{x},A} \boldsymbol{\nu}^k(t, \mathbf{x}, A) &= \left[\nabla_{\mathbf{x}} \boldsymbol{\nu}^k(t, \mathbf{x}, A) \quad \nabla_A \boldsymbol{\nu}^k(t, \mathbf{x}, A)\right] \in \mathbb{R}^{2\times(2+m)}, \\
\left\|\boldsymbol{\nu}^k(t, \cdot, \cdot)\right\|_{\mathbf{C^2}(\mathbb{R}^2\times\mathbb{R}^m;\mathbb{R}^2)} &= \left\|\boldsymbol{\nu}^k(t, \cdot, \cdot)\right\|_{\mathbf{L}^\infty(\mathbb{R}^2\times\mathbb{R}^m;\mathbb{R}^2)} + \left\|\nabla_{\mathbf{x},A} \boldsymbol{\nu}^k(t, \cdot, \cdot)\right\|_{\mathbf{L}^\infty(\mathbb{R}^2\times\mathbb{R}^m;\mathbb{R}^{2\times(2+m)})} \\
&\quad + \left\|\nabla^2_{\mathbf{x},\mathbf{x},A,A} \boldsymbol{\nu}^k(t, \cdot, \cdot)\right\|_{\mathbf{L}^\infty(\mathbb{R}^2\times\mathbb{R}^m;\mathbb{R}^{2\times(2+m)\times(2+m)})}.
\end{aligned}
$$

Also, for $\boldsymbol{\rho} \in \mathrm{BV}(\Omega; \mathbb{R}^N)$, we denote $\mathrm{TV}(\boldsymbol{\rho}) = \sum_{k=1}^{N} \mathrm{TV}(\rho^k)$.

We pose the following assumptions:

($\boldsymbol{\nu}$) For $k=1,\dots,N$, $\boldsymbol{\nu}^k \in (\mathbf{C^0}\cap\mathbf{L}^\infty)(I\times\mathbb{R}^2\times\mathbb{R}^m;\mathbb{R}^2)$; for all $t\in I$, $\boldsymbol{\nu}^k(t,\cdot,\cdot)\in\mathbf{C^2}(\mathbb{R}^2\times\mathbb{R}^m;\mathbb{R}^2)$ and $\left\|\boldsymbol{\nu}^k(t,\cdot,\cdot)\right\|_{\mathbf{C^2}(\mathbb{R}^2\times\mathbb{R}^m;\mathbb{R}^2)}$ is bounded uniformly in t and k, i.e. there exists a positive constant $\mathcal{V}$ such that $\left\|\boldsymbol{\nu}^k(t,\cdot,\cdot)\right\|_{\mathbf{C^2}(\mathbb{R}^2\times\mathbb{R}^m;\mathbb{R}^2)}\leq\mathcal{V}$ for all $t\in I$ and all $k=1,\dots,N$.

($\boldsymbol{\mathcal{J}}$) For $k=1,\dots,N$, $\mathcal{J}^k\colon \mathbf{L^1}(\mathbb{R}^2;\mathbb{R}^{N+1})\to\mathbf{C^2}(\mathbb{R}^2;\mathbb{R}^m)$ is such that there exists a positive K and a weakly increasing map $\mathcal{K}\in\mathbf{L^\infty_{loc}}(\mathbb{R}_+;\mathbb{R}_+)$ such that

($\boldsymbol{\mathcal{J}}$**.1**) for all $\boldsymbol{r}\in\mathbf{L^1}(\Omega;\mathbb{R}^{N+1})$

$$\begin{aligned}
\left\|\mathcal{J}^k[\boldsymbol{r}_\Omega]\right\|_{\mathbf{L}^\infty(\mathbb{R}^2;\mathbb{R}^m)} &\leq K\left\|\boldsymbol{r}_\Omega\right\|_{\mathbf{L^1}(\mathbb{R}^2;\mathbb{R}^{N+1})},\\
\left\|\nabla_{\mathbf{x}}\mathcal{J}^k[\boldsymbol{r}_\Omega]\right\|_{\mathbf{L}^\infty(\mathbb{R}^2;\mathbb{R}^{m\times 2})} &\leq K\left\|\boldsymbol{r}_\Omega\right\|_{\mathbf{L^1}(\mathbb{R}^2;\mathbb{R}^{N+1})},\\
\left\|\nabla^2_{\mathbf{x}}\mathcal{J}^k[\boldsymbol{r}_\Omega]\right\|_{\mathbf{L}^\infty(\mathbb{R}^2;\mathbb{R}^{m\times 2\times 2})} &\leq \mathcal{K}\left(\left\|\boldsymbol{r}_\Omega\right\|_{\mathbf{L^1}(\mathbb{R}^2;\mathbb{R}^{N+1})}\right)\left\|\boldsymbol{r}_\Omega\right\|_{\mathbf{L^1}(\mathbb{R}^2;\mathbb{R}^{N+1})},
\end{aligned}$$

($\boldsymbol{\mathcal{J}}$**.2**) for all $\boldsymbol{r}_1\in\mathbf{L^1}(\Omega_1;\mathbb{R}^{N+1})$ and $\boldsymbol{r}_2\in\mathbf{L^1}(\Omega_2;\mathbb{R}^{N+1})$

$$\begin{aligned}
\left\|\mathcal{J}^k[\boldsymbol{r}_{1,\Omega_1}]-\mathcal{J}^k[\boldsymbol{r}_{2,\Omega_2}]\right\|_{\mathbf{L}^\infty(\mathbb{R}^2;\mathbb{R}^m)} &\leq K\left\|\boldsymbol{r}_{1,\Omega_1}-\boldsymbol{r}_{2,\Omega_2}\right\|_{\mathbf{L^1}(\mathbb{R}^2;\mathbb{R}^{N+1})},\\
\left\|\nabla_{\mathbf{x}}\left(\mathcal{J}^k[\boldsymbol{r}_{1,\Omega_1}]-\mathcal{J}^k[\boldsymbol{r}_{2,\Omega_2}]\right)\right\|_{\mathbf{L}^\infty(\mathbb{R}^2;\mathbb{R}^{m\times N+1})} &\leq \mathcal{K}\left(\left\|\boldsymbol{r}_{1,\Omega_1}\right\|_{\mathbf{L^1}(\mathbb{R}^2;\mathbb{R}^{N+1})}\right)\left\|\boldsymbol{r}_{1,\Omega_1}-\boldsymbol{r}_{2,\Omega_2}\right\|_{\mathbf{L^1}(\mathbb{R}^2;\mathbb{R}^{N+1})},
\end{aligned}$$

where $\boldsymbol{r}_\Omega,\boldsymbol{r}_{1,\Omega_1},\boldsymbol{r}_{2,\Omega_2}$ are defined accordingly to (2). Above, Ω, Ω_1 and Ω_2 satisfy (**Ω.1**).

Solutions of problem (1) are then intended in the following weak sense.

Definition 1 [1, Def. 2.2],[2, Def. 2.1] *For any $T>0$ and $\boldsymbol{\rho}_0\in\mathbf{L^1}(\mathbb{R}^2,\Pi_{k=1}^N[0,R_k])$ such that* $\operatorname{supp}\boldsymbol{\rho}_0\subset\Omega$*, a function $\boldsymbol{\rho}\in\mathbf{C^0}([0,T],\mathbf{L^1}(\mathbb{R}^2;\Pi_{k=1}^N[0,R_k]))$ is said to be an* entropy weak solution *to* (1) *if, for $k=1,\dots,N$, setting $\boldsymbol{V}^k(t,\mathbf{x})=\boldsymbol{\nu}^k\left(t,\mathbf{x},\mathcal{J}^k[\boldsymbol{\rho}_\Omega(t)](\mathbf{x})\right)$, with $\boldsymbol{\rho}_\Omega$ defined as in* (2)*, ρ^k is a Kružkov entropy solution to the Cauchy problem*

$$\begin{cases}
\partial_t\rho^k+\operatorname{div}_{\mathbf{x}}\left[f_k\left(\rho^k\right)\boldsymbol{V}^k(t,\mathbf{x})\right]=0, & \mathbf{x}\in\mathbb{R}^2, t\geq 0,\\
\rho^k(0,\mathbf{x})=\rho_0^k(\mathbf{x}), & \mathbf{x}\in\mathbb{R}^2,
\end{cases}$$

i.e. for all $\kappa\in\mathbb{R}$ and all test functions $\phi\in\mathbf{C^\infty_c}(]-\infty,T[\times\mathbb{R}^2;\mathbb{R}_+)$ there holds

$$\begin{aligned}
&\int_0^T\int_{\mathbb{R}^2}\left\{\left|\rho^k-\kappa\right|\partial_t\phi+\operatorname{sgn}(\rho^k-\kappa)\left(f_k\left(\rho^k\right)-f_k(\kappa)\right)\boldsymbol{V}^k(t,\mathbf{x})\cdot\nabla_{\mathbf{x}}\phi\right\}\mathrm{d}\mathbf{x}\,\mathrm{d}t\\
&-\int_0^T\int_{\mathbb{R}^2}\operatorname{sgn}(\rho^k-\kappa)f_k(\kappa)\operatorname{div}_{\mathbf{x}}\boldsymbol{V}^k(t,\mathbf{x})\,\phi\;\mathrm{d}\mathbf{x}\,\mathrm{d}t+\int_{\mathbb{R}^2}\left|\rho_0^k(\mathbf{x})-\kappa\right|\phi(0,\mathbf{x})\,\mathrm{d}\mathbf{x}\geq 0.
\end{aligned}\tag{3}$$

The existence of solutions to (1) follows from [1, Theorem 2.3], see also [2, Theorem 2.2]. Notice that, unlike previous works such as [2, 5, 9], we consider different maximal densities R_k, $k=1,\dots,N$, for the different populations, allowing for larger modeling flexibility (e.g. regarding social distancing). The maximum principle still applies to each equation independently.

Theorem 1 *Let assumptions* $(\boldsymbol{\nu})$, $(\boldsymbol{\mathcal{J}})$, $(\boldsymbol{\Omega.1})$, $(\boldsymbol{\Omega.2})$, $(\boldsymbol{f})$ *hold. For any initial datum* $\boldsymbol{\rho}_0 \in \left(\mathbf{L^1} \cap \mathbf{L}^\infty \cap BV\right)(\Omega; \Pi_{k=1}^N [0, R_k])$, *there exists a solution* $\boldsymbol{\rho} \in \mathbf{C^0}(\mathbb{R}_+, \mathbf{L^1}(\Omega; \Pi_{k=1}^N [0, R_k]))$ *of* (1) *in the sense of Definition 1. Moreover, the following bounds hold*

$$\begin{aligned}
&\left\|\boldsymbol{\rho}(t,\cdot)\right\|_{\mathbf{L^1}(\Omega;\Pi_{k=1}^N[0,R_k])} = \|\boldsymbol{\rho}_0\|_{\mathbf{L^1}(\Omega;\Pi_{k=1}^N[0,R_k])},\\
&TV(\boldsymbol{\rho}(t,\cdot)) \leq e^{K_1 t}\, TV(\boldsymbol{\rho}_0) + K_2(e^{K_1 t} - 1),\\
&\left\|\boldsymbol{\rho}(t+\tau,\cdot) - \boldsymbol{\rho}(t,\cdot)\right\|_{\mathbf{L^1}(\Omega;\Pi_{k=1}^N[0,R_k])} \leq C(t)\tau,
\end{aligned}$$

where the constants K_1, K_2 *and the function* $C(t)$ *depend on* $\|\boldsymbol{\rho}_0\|_{\mathbf{L^1}}$, $TV(\boldsymbol{\rho}_0)$ *and on* f_k, $\boldsymbol{\nu}^k$, K *and* $\mathcal{K}$ *as in* $(\boldsymbol{\mathcal{J}})$, *for* $k = 1, \ldots, N$.

Remark 1 *If, instead of* $(\boldsymbol{f})$, *we assume*

$(\boldsymbol{f*})$ $f_k \in \left(\mathbf{C^2} \cap \mathbf{W^{2,\infty}}\right)(\mathbb{R}_+; \mathbb{R}_+)$ *with* $f_k(0) = 0$ *and* $\sup_r |f_k'(r)| < +\infty$ *for all* $k = 1, \ldots, N$,

existence of solutions to (1) *is still guaranteed. However, the maximum principle does not hold, namely, the* $\mathbf{L}^\infty$*-norm of the solution may increase exponentially in time, see [1, Theorem 2.3].*

The main result of this paper is the following, stating the stability of solutions to (1) with respect to the initial data and the domain boundaries.

Theorem 2 *Let assumptions* $(\boldsymbol{\nu})$, $(\boldsymbol{\mathcal{J}})$ *and* $(\boldsymbol{f})$ *hold. Let* $\Omega, \Theta \subseteq \mathbb{R}^2$ *satisfy* $(\boldsymbol{\Omega.1})$ *and let* $\boldsymbol{\nu}^k$ *satisfy* $(\boldsymbol{\Omega.2})$ *for both* Ω *and* Θ, *for* $k = 1, \ldots, N$. *Consider* $\boldsymbol{\rho}_0 \in \left(\mathbf{L^1} \cap \mathbf{L}^\infty \cap BV\right)(\Omega; \Pi_{k=1}^N [0, R_k])$ *and* $\boldsymbol{\sigma}_0 \in \left(\mathbf{L^1} \cap \mathbf{L}^\infty \cap BV\right)(\Theta; \Pi_{k=1}^N [0, R_k])$. *Call* $\boldsymbol{\rho}, \boldsymbol{\sigma}$ *the corresponding solutions to* (1), *defined respectively on the domains* Ω *and* Θ.

Then, for $t \in \mathbb{R}_+$, *the following estimate holds*

$$\left\|\boldsymbol{\rho}(t) - \boldsymbol{\sigma}(t)\right\|_{\mathbf{L^1}(\mathbb{R}^2;\Pi_{k=1}^N[0,R_k])} \leq \mathcal{K}_1(t)\|\boldsymbol{\rho}_0 - \boldsymbol{\sigma}_0\|_{\mathbf{L^1}(\mathbb{R}^2;\Pi_{k=1}^N[0,R_k])} + \mathcal{K}_2(t)\left\|\mu(\Omega^c) - \mu(\Theta^c)\right\|_{\mathbf{L^1}(\mathbb{R}^2;\mathbb{R})},$$

where the functions $\mathcal{K}_1(t)$ *and* $\mathcal{K}_2(t)$ *are respectively as in* (8) *and* (9) *and* μ *is defined in* (5).

We notice that the stability result above holds also if f satisfies $(\boldsymbol{f*})$. The statement of Theorem 2 should be changed accordingly to Remark 1, since the maximum principle does not hold.

Proof. We follow [32, Proposition 4.1], using Kružkov's *doubling of variables method* [28] in a form similar to [26, Theorem 1.3], adding the dependence on time to the spatial dependent part of the flux function, see also [6, Lemma 4] where the one-space-dimensional case is considered.

Introduce the following notation: for $k = 1, \ldots, N$ set

$$\boldsymbol{R}^k(t,\mathbf{x}) = \boldsymbol{\nu}^k\left(t, \mathbf{x}, \mathcal{J}^k[\boldsymbol{\rho}_\Omega(t)](\mathbf{x})\right), \qquad \boldsymbol{S}^k(t,\mathbf{x}) = \boldsymbol{\nu}^k\left(t, \mathbf{x}, \mathcal{J}^k[\boldsymbol{\sigma}_\Theta(t)](\mathbf{x})\right).$$

For each $k = 1, \ldots, N$, we follow the same steps of [32, Proposition 4.1], leading to

$$\begin{aligned}
\int_{\mathbb{R}^2} \left|\rho^k(t,\mathbf{x}) - \sigma^k(t,\mathbf{x})\right| \mathrm{d}\mathbf{x} \leq\ & \int_{\mathbb{R}^2} \left|\rho_0^k(\mathbf{x}) - \sigma_0^k(\mathbf{x})\right| \mathrm{d}\mathbf{x} \\
&+ \int_0^t \int_{\mathbb{R}^2} \left|\mathrm{div}\left(\boldsymbol{R}^k(s,\mathbf{x}) - \boldsymbol{S}^k(s,\mathbf{x})\right)\right| f_k\left(\rho^k(s,\mathbf{x})\right) \mathrm{d}\mathbf{x}\, \mathrm{d}s \\
&+ \left\|f_k'\right\|_\infty \int_0^t \left\|\boldsymbol{R}^k(s,\cdot) - \boldsymbol{S}^k(s,\cdot)\right\|_{\mathbf{L}^\infty(\mathbb{R}^2;\mathbb{R}^2)} \mathrm{TV}\left(\rho^k(s)\right) \mathrm{d}s\,,
\end{aligned} \tag{4}$$

where $t \in [0,T]$. By $(\boldsymbol{\nu})$ and $(\boldsymbol{\mathcal{J}}.\mathbf{2})$, we have

$$\begin{aligned}\left\|\boldsymbol{R}^k(s,\cdot)-\boldsymbol{S}^k(s,\cdot)\right\|_{\mathbf{L}^\infty(\mathbb{R}^2;\mathbb{R}^2)} &= \left\|\boldsymbol{\nu}^k\left(s,\cdot,\mathcal{J}^k[\boldsymbol{\rho}_\Omega(s)](\cdot)\right)-\boldsymbol{\nu}^k\left(s,\cdot,\mathcal{J}^k[\boldsymbol{\sigma}_\Theta(s)](\cdot)\right)\right\|_{\mathbf{L}^\infty(\mathbb{R}^2;\mathbb{R}^2)}\\ &\le \left\|\nabla_A\boldsymbol{\nu}^k\right\|_{\mathbf{L}^\infty(\Sigma_s)}\left\|\mathcal{J}^k[\boldsymbol{\rho}_\Omega(s)](\cdot)-\mathcal{J}^k[\boldsymbol{\sigma}_\Theta(s)](\cdot)\right\|_{\mathbf{L}^\infty(\mathbb{R}^2;\mathbb{R}^m)}\\ &\le \mathcal{V}K\left\|\boldsymbol{\rho}_\Omega(s,\cdot)-\boldsymbol{\sigma}_\Theta(s,\cdot)\right\|_{\mathbf{L}^1(\mathbb{R}^2;\mathbb{R}^{N+1})}.\end{aligned}$$

Moreover, by $(\boldsymbol{\nu})$, $(\boldsymbol{\mathcal{J}}.\mathbf{2})$ and $(\boldsymbol{f})$, we estimate

$$\begin{aligned}\left\|\operatorname{div}\left(\boldsymbol{R}^k(s,\cdot)-\boldsymbol{S}^k(s,\cdot)\right)\right\|_{\mathbf{L}^\infty(\mathbb{R}^2;\mathbb{R})} &\le \|\nabla_A\operatorname{div}_{\mathbf{x}}\boldsymbol{\nu}\|_{\mathbf{L}^\infty(\Sigma_s)}\left\|\mathcal{J}^k[\boldsymbol{\rho}_\Omega(s)](\cdot)-\mathcal{J}^k[\boldsymbol{\sigma}_\Theta(s)](\cdot)\right\|_{\mathbf{L}^\infty(\mathbb{R}^2;\mathbb{R}^m)}\\ &\quad+\|\nabla_A\boldsymbol{\nu}\|_{\mathbf{L}^\infty(\Sigma_s)}\left\|\nabla_{\mathbf{x}}\mathcal{J}^k[\boldsymbol{\rho}_\Omega(s)]-\nabla_{\mathbf{x}}\mathcal{J}^k[\boldsymbol{\sigma}_\Theta(s)]\right\|_{\mathbf{L}^\infty(\mathbb{R}^2;\mathbb{R}^{m\times 2})}\\ &\le \mathcal{V}K\left\|\boldsymbol{\rho}_\Omega(s,\cdot)-\boldsymbol{\sigma}_\Theta(s,\cdot)\right\|_{\mathbf{L}^1(\mathbb{R}^2;\mathbb{R}^{N+1})}\\ &\quad+\mathcal{V}\mathcal{K}\left(\left\|\boldsymbol{\rho}_\Omega(s,\cdot)\right\|_{\mathbf{L}^1(\mathbb{R}^2)}\right)\left\|\boldsymbol{\rho}_\Omega(s,\cdot)-\boldsymbol{\sigma}_\Theta(s,\cdot)\right\|_{\mathbf{L}^1(\mathbb{R}^2;\mathbb{R}^{N+1})},\end{aligned}$$

since

$$\begin{aligned}&\operatorname{div}\left(\boldsymbol{R}^k(s,\mathbf{x})-\boldsymbol{S}^k(s,\mathbf{x})\right)\\ =\;&\operatorname{div}_{\mathbf{x}}\left(\boldsymbol{\nu}^k\left(s,\mathbf{x},\mathcal{J}^k[\boldsymbol{\rho}_\Omega(s)](\mathbf{x})\right)-\boldsymbol{\nu}^k\left(s,\mathbf{x},\mathcal{J}^k[\boldsymbol{\sigma}_\Theta(s)](\mathbf{x})\right)\right)\\ &+\nabla_A\nu_1^k(s,\mathbf{x},\mathcal{J}^k[\boldsymbol{\rho}_\Omega(s)](\mathbf{x}))\cdot\partial_{x_1}\mathcal{J}^k[\boldsymbol{\rho}_\Omega(s)](\mathbf{x})+\nabla_A\nu_2^k(s,\mathbf{x},\mathcal{J}^k[\boldsymbol{\rho}_\Omega(s)](\mathbf{x}))\cdot\partial_{x_2}\mathcal{J}^k[\boldsymbol{\rho}_\Omega(s)](\mathbf{x})\\ &-\nabla_A\nu_1^k(s,\mathbf{x},\mathcal{J}^k[\boldsymbol{\sigma}_\Theta(s)](\mathbf{x}))\cdot\partial_{x_1}\mathcal{J}^k[\boldsymbol{\sigma}_\Theta(s)](\mathbf{x})-\nabla_A\nu_2^k(s,\mathbf{x},\mathcal{J}^k[\boldsymbol{\sigma}_\Theta(s)](\mathbf{x}))\cdot\partial_{x_2}\mathcal{J}^k[\boldsymbol{\sigma}_\Theta(s)](\mathbf{x}).\end{aligned}$$

Observe that

$$\left\|(\boldsymbol{\rho}_\Omega-\boldsymbol{\sigma}_\Theta)(s,\cdot)\right\|_{\mathbf{L}^1(\mathbb{R}^2;\mathbb{R}^{N+1})}=\left\|(\boldsymbol{\rho}-\boldsymbol{\sigma})(s,\cdot)\right\|_{\mathbf{L}^1(\mathbb{R}^2;\mathbb{R}^N)}+\left\|\mu(\Omega^c)-\mu(\Theta^c)\right\|_{\mathbf{L}^1(\mathbb{R}^2;\mathbb{R})},$$

where

$$\mu(\Omega^c):=\sum_{\ell=1}^{M_\Omega}R_{N+\ell}\chi_{\Omega_\ell^c},\qquad \mu(\Theta^c):=\sum_{\ell=1}^{M_\Theta}\tilde{R}_{N+\ell}\chi_{\Theta_\ell^c},\tag{5}$$

and M_Ω and M_Θ are the numbers of connected components of Ω^c and Θ^c, respectively. Indeed

$$\begin{aligned}\sum_{k=1}^{N+1}\int_{\mathbb{R}^2}\left|(\rho_\Omega^k-\sigma_\Theta^k)(s,\mathbf{x})\right|\mathrm{d}\mathbf{x} &= \sum_{k=1}^{N}\int_{\mathbb{R}^2}\left|(\rho^k-\sigma^k)(s,\mathbf{x})\right|\mathrm{d}\mathbf{x}\\ &\quad+\int_{\mathbb{R}^2}\left|\left(\sum_{\ell=1}^{M_\Omega}R_{N+\ell}\chi_{\Omega_\ell^c}-\sum_{\ell=1}^{M_\Theta}\tilde{R}_{N+\ell}\chi_{\Theta_\ell^c}\right)(s,\mathbf{x})\right|\mathrm{d}\mathbf{x}\,.\end{aligned}$$

Therefore, from (4) and the total variation estimate in Theorem 1, we get

$$\left\|\rho^k(t,\cdot)-\sigma^k(t,\cdot)\right\|_{\mathbf{L}^1(\mathbb{R}^2;\mathbb{R})}\le\left\|\rho_0^k-\sigma_0^k\right\|_{\mathbf{L}^1(\mathbb{R}^2;\mathbb{R})}+\left\|\mu(\Omega^c)-\mu(\Theta^c)\right\|_{\mathbf{L}^1(\mathbb{R}^2;\mathbb{R})}\int_0^t\widetilde{\mathcal{K}}(s)\,\mathrm{d}s\tag{6}$$

$$+\int_0^t \widetilde{\mathcal{K}}(s)\big\|(\boldsymbol{\rho}-\boldsymbol{\sigma})(s,\cdot)\big\|_{\mathbf{L^1}(\mathbb{R}^2;\mathbb{R}^N)}\,\mathrm{d}s\,,$$

where $\widetilde{\mathcal{K}}(s) := \max_k \widetilde{\mathcal{K}}_k(s)$ with

$$\widetilde{\mathcal{K}}_k(s) := \mathcal{V}\|f_k'\|_\infty\Bigg[\Big\|\rho_0^k\Big\|_{\mathbf{L^1}(\mathbb{R}^2;\mathbb{R})}\left(K+\mathcal{K}\left(\|\boldsymbol{\rho}_0\|_{\mathbf{L^1}(\mathbb{R}^2;\mathbb{R}^N)}+\big\|\mu(\Omega^c)\big\|_{\mathbf{L^1}(\mathbb{R}^2;\mathbb{R})}\right)\right)$$
$$+K\left(e^{K_1 s}\mathrm{TV}(\boldsymbol{\rho}_0)+K_2(e^{K_1 s}-1)\right)\Bigg].$$

Now we sum over k in (6) obtaining

$$\big\|\boldsymbol{\rho}(t,\cdot)-\boldsymbol{\sigma}(t,\cdot)\big\|_{\mathbf{L^1}(\mathbb{R}^2;\mathbb{R}^N)} \le \|\boldsymbol{\rho}_0-\boldsymbol{\sigma}_0\|_{\mathbf{L^1}(\mathbb{R}^2;\mathbb{R}^N)}+N\big\|\mu(\Omega^c)-\mu(\Theta^c)\big\|_{\mathbf{L^1}(\mathbb{R}^2;\mathbb{R})}\int_0^t \widetilde{\mathcal{K}}(s)\,\mathrm{d}s \tag{7}$$
$$+N\int_0^t \widetilde{\mathcal{K}}(s)\big\|(\boldsymbol{\rho}-\boldsymbol{\sigma})(s,\cdot)\big\|_{\mathbf{L^1}(\mathbb{R}^2;\mathbb{R}^N)}\,\mathrm{d}s\,.$$

Applying Gronwall's Lemma, we derive the desired estimate

$$\big\|\boldsymbol{\rho}(t,\cdot)-\boldsymbol{\sigma}(t,\cdot)\big\|_{\mathbf{L^1}(\mathbb{R}^2;\mathbb{R}^N)} \le \|\boldsymbol{\rho}_0-\boldsymbol{\sigma}_0\|_{\mathbf{L^1}(\mathbb{R}^2;\mathbb{R}^N)}e^{N\int_0^t \widetilde{\mathcal{K}}(s)\mathrm{d}s}$$
$$+N\big\|\mu(\Omega^c)-\mu(\Theta^c)\big\|_{\mathbf{L^1}(\mathbb{R}^2;\mathbb{R})}\int_0^t \widetilde{\mathcal{K}}(s)e^{N\int_s^t \widetilde{\mathcal{K}}(r)\mathrm{d}r}\,\mathrm{d}s\,.$$

We can set

$$\mathcal{K}_1(t) := e^{N\int_0^t \widetilde{\mathcal{K}}(s)\mathrm{d}s} \tag{8}$$

and

$$\mathcal{K}_2(t) := N\int_0^t \widetilde{\mathcal{K}}(s)e^{N\int_s^t \widetilde{\mathcal{K}}(r)\mathrm{d}r}\,\mathrm{d}s \tag{9}$$

to get

$$\big\|\boldsymbol{\rho}(t,\cdot)-\boldsymbol{\sigma}(t,\cdot)\big\|_{\mathbf{L^1}(\mathbb{R}^2;\mathbb{R}^N)} \le \mathcal{K}_1(t)\|\boldsymbol{\rho}_0-\boldsymbol{\sigma}_0\|_{\mathbf{L^1}(\mathbb{R}^2;\mathbb{R}^N)}+\mathcal{K}_2(t)\big\|\mu(\Omega^c)-\mu(\Theta^c)\big\|_{\mathbf{L^1}(\mathbb{R}^2;\mathbb{R})}.$$

□

Remark 2 As a byproduct, the above stability result guarantees the existence of optimal solutions of minimization or maximization problems involving density dependent functionals of the form

$$\mathcal{F}(\boldsymbol{\rho}_0,\Omega) := \int_0^T\int_{\mathbb{R}^2}\Psi(\boldsymbol{\rho}(t,\mathbf{x}))\,\mathrm{d}\mathbf{x}\,\mathrm{d}t\,,\qquad T\in\mathbb{R}_+, \tag{10}$$

where $\Psi\in(\mathbf{C^0}\cap\mathbf{L^1})(\mathbb{R}^N;\mathbb{R}_+)$ and $\boldsymbol{\rho}\in\mathbf{C^0}(\mathbb{R}_+;\mathbf{L^1}(\Omega;\mathbb{R}^N_+))$ is the entropy weak solution of (1).

2.1 A particular example

A possible choice for the nonlocal vector field is the following:

$$\boldsymbol{\nu}^k\left(t,\mathbf{x},\mathcal{J}^k[\boldsymbol{\rho}_\Omega(t)](\mathbf{x})\right) = \left(1-\varepsilon_1\,\mathcal{I}_1^k[\boldsymbol{\rho}_\Omega(t)](\mathbf{x})\right)\boldsymbol{u}^k(\mathbf{x})-\varepsilon_2\,\mathcal{I}_2^k[\nabla\boldsymbol{\rho}_\Omega(t)](\mathbf{x}), \tag{11}$$

where $\boldsymbol{u}^k : \Omega \to \mathbb{R}^2$ are the (normalized) fixed smooth vector fields of preferred directions. Here, the nonlocal operator $\mathcal{J}^k$ is composed of two parts:

$$\mathcal{I}_1^k[\boldsymbol{\rho}_\Omega(t)] = \mathcal{I}_k\left[\sum_{h=1}^{N+1} \rho_\Omega^h(t,\cdot)\right], \quad \mathcal{I}_2^k[\nabla\boldsymbol{\rho}_\Omega(t)] = \mathcal{I}_k\left[\nabla \sum_{\substack{h=1\\h\neq k}}^{N+1} \rho_\Omega^h(t,\cdot)\right], \tag{12}$$
$$\text{with } \mathcal{I}_k[\rho] := \frac{\eta_k * \rho}{\sqrt{1+\|\eta_k * \rho\|^2}},$$

where η_k, $k = 1, \dots, N$, are smooth non-negative kernels with compact support such that

$$\iint_{\mathbb{R}^2} \eta_k(\mathbf{x})\, \mathrm{d}\mathbf{x} = 1.$$

Formulas (11)–(12) indicate that the k-th population adjusts its preferred direction of movement $\boldsymbol{u}^k$ twofold: the scalar term $\mathcal{I}_1^k$ takes into account the average total density (including obstacles) around $\mathbf{x}$, thus acting on the speed of the movement, while the vector term $\mathcal{I}_2^k$ describes the tendency of individuals of the k-th population to avoid regions with high (average) density gradient of the other populations (including obstacles), thus acting on the direction of movement. The coefficients $\varepsilon_1 > 0$ and $\varepsilon_2 > 0$ are scaling factors, which temper the impact of the correction terms.
In particular, in the case $N = 2$, we can consider the following model (similarly to what studied in [18]):

$$\begin{cases} \partial_t\rho^1 + \mathrm{div}_{\mathbf{x}}\left[\rho^1 v_1(\rho^1)\left(\left(1-\varepsilon_1\mathcal{I}_1[\rho^1+\rho^2+\rho^3]\right)\boldsymbol{u}^1(\mathbf{x}) - \varepsilon_2\mathcal{I}_1[\nabla(\rho^2+\rho^3)]\right)\right] = 0, \\ \partial_t\rho^2 + \mathrm{div}_{\mathbf{x}}\left[\rho^2 v_2(\rho^2)\left(\left(1-\varepsilon_1\mathcal{I}_2[\rho^1+\rho^2+\rho^3]\right)\boldsymbol{u}^2(\mathbf{x}) - \varepsilon_2\mathcal{I}_2[\nabla(\rho^1+\rho^3)]\right)\right] = 0, \end{cases} \tag{13}$$

where, for $k = 1, 2$, $v_k > 0$ are the pedestrians' speed functions and $\rho^3 = \sum_{\ell=1}^{M} R_{2+\ell}\chi_{\Omega_\ell^c}$ represents the (fixed) obstacle density.

Remark 3 Note that, even in the worst case scenario $\boldsymbol{u}^k(\mathbf{x}) = \mathbf{n}(\mathbf{x})$ for some $\mathbf{x} \in \partial\Omega$, one can find R_ℓ big enough to guarantee (**Ω.2**), provided that $1 < \varepsilon_1 + \varepsilon_2$.

To match the general hypotheses ($\boldsymbol{f}$), ($\boldsymbol{\nu}$) and ($\boldsymbol{\mathcal{J}}$), we need:

(v) $v_k \in \left(\mathbf{C^2} \cap \mathbf{W^{2,\infty}}\right)(\mathbb{R}_+;\mathbb{R}_+)$ with $v_k(R_k) = 0$ for $k = 1, 2$.

($\boldsymbol{u}$) $\boldsymbol{u}^k \in (\mathbf{C^2} \cap \mathbf{W^{2,\infty}})(\mathbb{R}^2;\mathbb{R}^2)$ for $k = 1, 2$.

(η) $\eta_k \in (\mathbf{C_c^3} \cap \mathbf{W^{3,\infty}})(\mathbb{R}^2;\mathbb{R}_+)$ for $k = 1, 2$.

3 Differentiability

In this section, we assume $f_k(\rho^k) = \rho^k$ for $k = 1, \dots, N$, that is, we have a system of linear transport equations as in [8]. We are interested in the differentiability of the solution $\boldsymbol{\rho}$ with respect to the obstacle positions. More precisely, we consider a vector field $\boldsymbol{\omega} \in \mathbf{C^1_{loc}}(\mathbb{R}^2;\mathbb{R}^2)$ and the solution of the differential equation

$$\dot{X}(h,\mathbf{x}) = \boldsymbol{\omega}(X(h,\mathbf{x})) \ \text{ for } h \geq 0, \qquad X(0,\mathbf{x}) = \mathbf{x},$$

which generates the family of transformations $\left\{T^h_{\boldsymbol{\omega}} : \mathbb{R}^2 \to \mathbb{R}^2 \colon h \geq 0\right\}$ defined by $T^h_{\boldsymbol{\omega}}(\mathbf{x}) := X(h, \mathbf{x})$ [14, Chapter 9]. Setting $\Omega^h := T^h_{\boldsymbol{\omega}}(\Omega)$ to be the perturbation of the original domain through the vector field $\boldsymbol{\omega}$, let $\boldsymbol{\rho}$ be the solution of

$$\begin{cases} \partial_t \rho^k + \operatorname{div}_{\mathbf{x}} \left[\rho^k \boldsymbol{\nu}^k \left(t, \mathbf{x}, \mathcal{J}^k[\boldsymbol{\rho}_\Omega] \right) \right] = 0, & \mathbf{x} \in \mathbb{R}^2, t \geq 0,\ k = 1, \dots, N, \\ \boldsymbol{\rho}(0, \mathbf{x}) = \boldsymbol{\rho}_0(\mathbf{x}), & \mathbf{x} \in \mathbb{R}^2, \end{cases} \tag{14}$$

and $\boldsymbol{\rho}^h$ the solution of

$$\begin{cases} \partial_t \rho^k + \operatorname{div}_{\mathbf{x}} \left[\rho^k \boldsymbol{\nu}^k \left(t, \mathbf{x}, \mathcal{J}^k[\boldsymbol{\rho}_{\Omega^h}] \right) \right] = 0, & \mathbf{x} \in \mathbb{R}^2, t \geq 0,\ k = 1, \dots, N, \\ \boldsymbol{\rho}(0, \mathbf{x}) = \boldsymbol{\rho}_0(\mathbf{x}), & \mathbf{x} \in \mathbb{R}^2. \end{cases} \tag{15}$$

Then the Gâteaux derivative is given by

$$\boldsymbol{r} := \lim_{h \to 0} \frac{\boldsymbol{\rho}^h - \boldsymbol{\rho}}{h} \qquad \text{strongly in } \mathbf{L^1},$$

which (formally) solves

$$\begin{cases} \partial_t r^k + \operatorname{div}_{\mathbf{x}} \left[r^k \boldsymbol{\nu}^k \left(t, \mathbf{x}, \mathcal{J}^k[\boldsymbol{\rho}_\Omega] \right) + \rho^k \nabla_A \boldsymbol{\nu}^k \left(t, \mathbf{x}, \mathcal{J}^k[\boldsymbol{\rho}_\Omega] \right) D_{\boldsymbol{\omega}} \mathcal{J}^k[\boldsymbol{\rho}_\Omega][\boldsymbol{r}] \right] = 0, \\ \boldsymbol{r}(0, \mathbf{x}) = 0, \end{cases} \tag{16}$$

for $\mathbf{x} \in \mathbb{R}^2$, $t \geq 0$, $k = 1, \dots, N$. Remembering (2), the above derivative is defined as

$$D_{\boldsymbol{\omega}} \mathcal{J}^k[\boldsymbol{\rho}_\Omega][\boldsymbol{r}] := D\mathcal{J}^k[\boldsymbol{\rho}_\Omega] \begin{bmatrix} \boldsymbol{r} \\ \sum_{\ell=1}^M R_{N+\ell} \nabla \chi_{\Omega^c_\ell} \cdot \boldsymbol{\omega} \end{bmatrix} = D\mathcal{J}^k[\boldsymbol{\rho}_\Omega] \begin{bmatrix} \boldsymbol{r} \\ \sum_{\ell=1}^M R_{N+\ell} \mathbf{n} \cdot \boldsymbol{\omega} \chi_{\partial\Omega^c_\ell} \end{bmatrix}.$$

(With slight abuse of notation since $\mathbf{n}$ is defined only on $\partial\Omega$.)

Note that

$$\rho^k \nabla_A \boldsymbol{\nu}^k \left(t, \mathbf{x}, \mathcal{J}^k[\boldsymbol{\rho}_\Omega] \right) D_{\boldsymbol{\omega}} \mathcal{J}^k[\boldsymbol{\rho}_\Omega][\boldsymbol{r}] \equiv 0$$

in Ω^c, since $\rho^k(t, \mathbf{x}) = 0$ for $\mathbf{x} \in \Omega^c$, $t \geq 0$. Therefore, by (**Ω.2**), we ensure $\boldsymbol{r}^k(t, \mathbf{x}) = 0$ for $\mathbf{x} \in \Omega^c$, $t \geq 0$.

Following [8, 9], we note that (16) has the form

$$\begin{cases} \partial_t r^k + \operatorname{div}_{\mathbf{x}} \left(r^k \boldsymbol{a}^k(t, \mathbf{x}) + \boldsymbol{b}^k(t, \mathbf{x}) \right) = 0, \\ r^k(0, \mathbf{x}) = 0, \end{cases} \tag{17}$$

where $\boldsymbol{a}^k(t, \mathbf{x}) = \boldsymbol{\nu}^k \left(t, \mathbf{x}, \mathcal{J}^k[\boldsymbol{\rho}_\Omega] \right) \in \mathbb{R}^2$ and $\boldsymbol{b}^k(t, \mathbf{x}) = \rho^k \nabla_A \boldsymbol{\nu}^k \left(t, \mathbf{x}, \mathcal{J}^k[\boldsymbol{\rho}_\Omega] \right) D_{\boldsymbol{\omega}} \mathcal{J}^k[\boldsymbol{\rho}_\Omega][\boldsymbol{r}] \in \mathbb{R}^2$. In turn, (17) can be rewritten as

$$\begin{cases} \partial_t r^k + \operatorname{div}_{\mathbf{x}} \left(r^k \boldsymbol{a}^k(t, \mathbf{x}) \right) = - \operatorname{div}_{\mathbf{x}} \boldsymbol{b}^k(t, \mathbf{x}), \\ r^k(0, \mathbf{x}) = 0. \end{cases} \tag{18}$$

Setting $B^k(t,\mathbf{x}) = -\operatorname{div}_{\mathbf{x}} \boldsymbol{b}^k(t,\mathbf{x})$ and referring to [8, Lemma 5.1], existence and uniqueness of entropy weak solutions for (17) requires the following regularity of $\boldsymbol{a}^k$ and B^k:

$$\boldsymbol{a}^k \in (\mathbf{C^0} \cap \mathbf{L}^\infty)([0,T[\,\times\mathbb{R}^2;\mathbb{R}^2), \tag{19a}$$

$$\boldsymbol{a}^k(t,\cdot) \in \mathbf{C^1}(\mathbb{R}^2;\mathbb{R}^2) \quad \forall t \in [0,T[\,, \tag{19b}$$

$$\nabla_{\mathbf{x}} \boldsymbol{a}^k \in \mathbf{L}^\infty([0,T[\,\times\mathbb{R}^2;\mathbb{R}^{2\times 2}), \tag{19c}$$

$$B^k \in \mathbf{L}^\infty([0,T[;\mathbf{L^1}(\mathbb{R}^2;\mathbb{R})) \cap \mathbf{L}^\infty([0,T[\,\times\mathbb{R}^2;\mathbb{R}), \tag{19d}$$

and for the initial datum $r^k(0,\cdot) \in (\mathbf{L^1} \cap \mathbf{L}^\infty)(\mathbb{R}^2;\mathbb{R})$. Observe that

- (19a) is guaranteed by $(\boldsymbol{\nu})$ and $(\boldsymbol{\mathcal{J}})$; indeed, the required regularity of $\mathcal{J}^k[\boldsymbol{\rho}] = \Big(\mathcal{J}^k[\boldsymbol{\rho}(t)]\Big)(\mathbf{x})$ with respect to t derives from $(\boldsymbol{\mathcal{J}}.\mathbf{2})$ and the $\mathbf{L^1}$ Lipschitz continuous dependence in time given by Theorem 1;
- (19b) follows as well from $(\boldsymbol{\nu})$ and $(\boldsymbol{\mathcal{J}})$: indeed it is $\boldsymbol{a}^k(t,\cdot) \in \mathbf{C^2}(\mathbb{R}^2;\mathbb{R}^2)$;
- in (19c), we have $\nabla_{\mathbf{x}} \boldsymbol{a}^k = \nabla_{\mathbf{x}} \boldsymbol{\nu}^k + \nabla_A \boldsymbol{\nu}^k \nabla_{\mathbf{x}} \mathcal{J}^k[\boldsymbol{\rho}_\Omega]$, so $\nabla_{\mathbf{x}} \boldsymbol{\nu}^k, \nabla_A \boldsymbol{\nu}^k \in \mathbf{L}^\infty([0,T[\,\times\mathbb{R}^2;\mathbb{R}^{2\times 2})$ is guaranteed by $(\boldsymbol{\nu})$, while $\nabla_{\mathbf{x}} \mathcal{J}^k[\boldsymbol{\rho}_\Omega] \in \mathbf{L}^\infty([0,T[\,\times\mathbb{R}^2;\mathbb{R}^{2\times 2})$ is ensured by $(\boldsymbol{\mathcal{J}}.\mathbf{1})$;
- for (19d), if we assume that $\boldsymbol{\rho}_0$ has compact support, then by finite propagation speed also $\boldsymbol{\rho}(t,\cdot)$ has compact support for all $t > 0$; therefore, it is enough to require $\operatorname{div}_{\mathbf{x}} \rho^k$, $\operatorname{div}_{\mathbf{x}} \nabla_A \boldsymbol{\nu}^k$ and $\operatorname{div}_{\mathbf{x}} D_{\boldsymbol{\omega}} \mathcal{J}^k[\boldsymbol{\rho}_\Omega][\boldsymbol{r}]$ to be in $\mathbf{L}^\infty([0,T[\,\times\mathbb{R}^2;\mathbb{R})$; for $\operatorname{div}_{\mathbf{x}} \nabla_A \boldsymbol{\nu}^k$, this is guaranteed by $(\boldsymbol{\nu})$; for $\operatorname{div}_{\mathbf{x}} \rho^k$, we need $\rho^k \in \mathbf{W^{1,\infty}}(\Omega;\mathbb{R}^N)$, and this is guaranteed by [8, Proposition 2.5] if we take $\boldsymbol{\rho}_0 \in \mathbf{W^{1,\infty}}(\Omega;\Pi_{k=1}^N[0,R_k])$; finally, for $\operatorname{div}_{\mathbf{x}} D_{\boldsymbol{\omega}} \mathcal{J}^k[\boldsymbol{\rho}_\Omega][\boldsymbol{r}]$, we need $D_{\boldsymbol{\omega}} \mathcal{J}^k[\boldsymbol{\rho}_\Omega][\boldsymbol{r}] \in \mathbf{W^{1,\infty}}$ which is satisfied by $(\boldsymbol{\mathcal{J}}.\mathbf{1})$.

Therefore, as in[9, Theorem 2.2], we can state the following differentiability result.

Theorem 3 *Let assumptions $(\boldsymbol{\nu})$, $(\boldsymbol{\mathcal{J}})$, $(\boldsymbol{\Omega}.\boldsymbol{1})$ and $(\boldsymbol{\Omega}.\boldsymbol{2})$ hold. Let $\boldsymbol{\rho}_0 \in \mathbf{W^{1,\infty}}(\Omega;\Pi_{k=1}^N[0,R_k])$ and $\boldsymbol{\omega} \in \mathbf{C^1_{loc}}(\mathbb{R}^2;\mathbb{R}^2)$. Then, for all $t > 0$, the solution $\boldsymbol{\rho} \in \mathbf{C^0}(\mathbb{R}_+;\mathbf{L^1}(\Omega;\mathbb{R}_+^N))$ of (14) is strongly $\mathbf{L^1}$ Gâteaux differentiable in the direction $\boldsymbol{\omega}$ and the Gâteaux derivative $\boldsymbol{r} \in \mathbf{C^0}(\mathbb{R}_+;\mathbf{L^1}(\Omega;\mathbb{R}_+^N))$ is the (entropy) weak solution of the sensitivity equation (16).*

A direct chain rule calculation gives the following necessary condition for optimality.

Corollary 4 *Let us consider the problem of minimizing (or maximizing) a functional of the form*

$$J(\Omega) := \int_0^{+\infty} \int_{\mathbb{R}^2} \Psi(\boldsymbol{\rho}(t,\mathbf{x}))\,\mathrm{d}\mathbf{x}\,\mathrm{d}t\,, \tag{20}$$

where $\Psi \in \mathbf{C^{1,1}}(\mathbb{R}^N;\mathbb{R}_+)$ and $\boldsymbol{\rho} \in \mathbf{C^0}(\mathbb{R}_+;\mathbf{L^1}(\Omega;\mathbb{R}_+^N))$ is the solution of (14).
If Ω is optimal, then

$$D_{\boldsymbol{\omega}} J(\Omega) = \int_0^{+\infty} \int_{\mathbb{R}^2} \nabla\Psi(\boldsymbol{\rho}(t,\mathbf{x})) \cdot \boldsymbol{r}(t,\mathbf{x})\,\mathrm{d}\mathbf{x}\,\mathrm{d}t = 0, \tag{21}$$

where $\boldsymbol{r} \in \mathbf{C^0}(\mathbb{R}_+;\mathbf{L^1}(\Omega;\mathbb{R}_+^N))$ solves (16).

4 Numerical tests

To illustrate the previous results in a specific application example, we consider a sample situation where two populations, represented by their densities ρ^1 and ρ^2, evacuate from a domain consisting of two perpendicular intersecting corridors, similarly to [18, Section 4.2] and [17, Section 4.3.1]. In particular, we aim at minimizing the evacuation time from the domain by finding the optimal position of a square obstacle, later denoted by Ω_1^c, in the intersection area.

For the numerical integrations, we exploit a modified Lax-Friedrichs scheme [4] with dimensional splitting. In order to consider the differentiability, we set $f_k(\rho) = \rho$ for $k = 1, 2$, so that (13) reads

$$\begin{cases} \partial_t \rho^1 + \mathrm{div}_{\mathbf{x}} \left[\rho^1 \left(\left(1 - \varepsilon_1 \mathcal{I}_1[\rho^1 + \rho^2 + \rho^3]\right) \boldsymbol{u}^1(\mathbf{x}) - \varepsilon_2 \mathcal{I}_1[\nabla(\rho^2 + \rho^3)] \right) \right] = 0, \\ \partial_t \rho^2 + \mathrm{div}_{\mathbf{x}} \left[\rho^2 \left(\left(1 - \varepsilon_1 \mathcal{I}_2[\rho^1 + \rho^2 + \rho^3]\right) \boldsymbol{u}^2(\mathbf{x}) - \varepsilon_2 \mathcal{I}_2[\nabla(\rho^1 + \rho^3)] \right) \right] = 0, \end{cases} \tag{22}$$

where $\rho^3 = R\,\chi_{\Omega_1^c}$ represents the (fixed) obstacle density. The walking domain is

$$\Omega =]-3, 3[\times]-0.5, 0.5[\cup]-0.5, 0.5[\times]-3, 3[\setminus \Omega_1^c$$

where the exits are located at $\Gamma_1 = \{3\} \times]-0.5, 0.5[$ and $\Gamma_2 =]-0.5, 0.5[\times \{3\}$ and

$$\Omega_1^c =]x_1^o, x_1^o + s[\times]x_2^o, x_2^o + s[,$$

the fixed side of the square obstacle being $s = 0.25$, its lower left corner (x_1^o, x_2^o) belonging to the set of admissible obstacle positions $\Omega_{\mathrm{obs}} := [-0.5, 0.25[\times [-0.8, 0.25[\cup [-0.8, 0.5] \times [-0.5, 0.25[$, see Figure 1. Notice that, with this choice of Ω_{obs}, the obstacle may both lie entirely at the intersection of the two corridors, and, with reference to one or the other population, be placed also in the incoming corridor. The same density R is also considered in the four walls delimiting the corridors: $[0.5, 3] \times [0.5, 3]$, $[0.5, 3] \times [-3, -0.5]$, $[-3, -0.5] \times [-3, -0.5]$ and $[-3, -0.5] \times [0.5, 3]$.

The given normalized vector fields $\boldsymbol{u}^1$ and $\boldsymbol{u}^2$, pointing towards the respective exits, are depicted in Figure 1. We remark that they do not take into consideration the presence of the obstacle and are therefore independent of its position. The other parameters and the kernel functions are the following:

$$R = 2, \quad \varepsilon_1 = 0.8, \quad \varepsilon_2 = 0.9, \quad \eta_1(\mathbf{x}) = \eta_2(\mathbf{x}) = \begin{cases} \frac{128\pi}{315}(0.2)^{18}(0.2^4 - \|\mathbf{x}\|^4)^4 & \text{if } \|\mathbf{x}\| \le 0.2, \\ 0 & \text{if } \|\mathbf{x}\| > 0.2. \end{cases}$$

The initial datum is the following, see also Figure 1,

$$\rho_0^1(\mathbf{x}) = 0.95\chi_{]-2.35,-1.65[\times]-0.25,0.25[}(\mathbf{x}), \qquad \rho_0^2(\mathbf{x}) = 0.3\chi_{]-0.25,0.25[\times]-2.35,-1.65[}(\mathbf{x}),$$

so that the total mass in the domain at the initial time is $\left\|\rho_0^1 + \rho_0^2\right\|_{\mathbf{L^1}(\Omega)} = 0.4375$.
Numerical solutions are computed on a uniform Cartesian mesh grid with 768×768 points, that is $\Delta x_1 = \Delta x_2 = 5/600$.

Aiming to find the optimal position of the obstacle, which minimizes the total travel time, we consider the cost functional (20) with $\Psi(\boldsymbol{\rho}) = \sum_{k=1}^M \rho^k$, that is

$$J(x_1^o, x_2^o) = \int_0^\infty \int_\Omega \left(\rho^1(t, \mathbf{x}) + \rho^2(t, \mathbf{x}) \right) \mathrm{d}\mathbf{x}\, \mathrm{d}t\,.$$

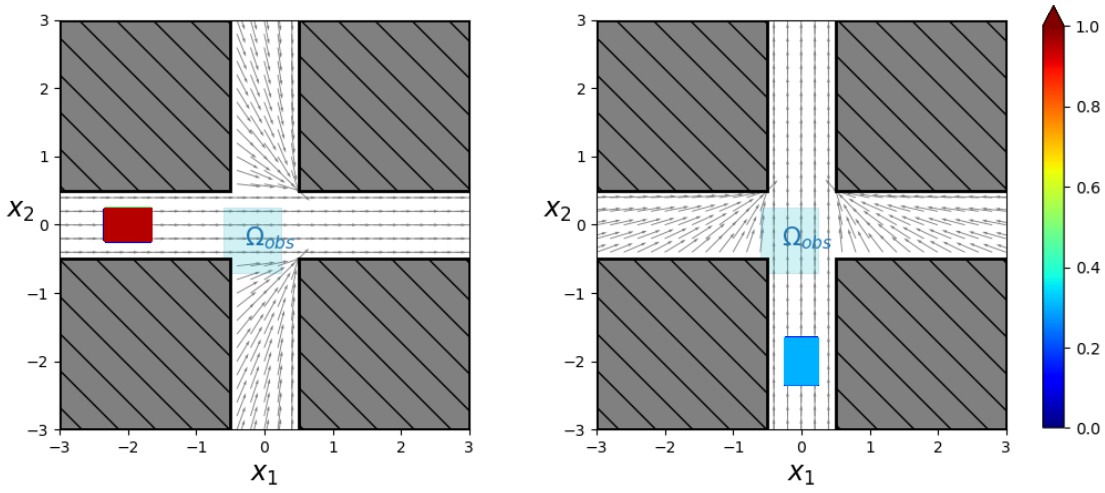

Figure 1: Left: initial datum ρ_0^1 and vector field $\boldsymbol{u}^1$. Right: initial datum ρ_0^2 and vector field $\boldsymbol{u}^2$. In each picture, we highlight the area Ω_{obs} where the lower left corner (x_1^o, x_2^o) of the obstacle may be located.

Numerically, the time integral is computed on the interval $[0, T_{\text{ev}}]$, where T_{ev} is the evacuation time, in the sense that the integration stops as soon as $\left\|\rho^1(T_{\text{ev}}, \cdot) + \rho^2(T_{\text{ev}}, \cdot)\right\|_{\mathbf{L^1}(\Omega)} < 10^{-3}$.
As reference, we consider the evacuation without obstacle at the intersection, i.e. $\Omega_1^c = \emptyset$, which leads to $T_{\text{ref}} = 14.375$. This solution is displayed in Figure 2 at different times.

To locate the minima, we perform around 124 numerical simulations, letting the position of the lower left corner of the obstacle vary inside Ω_{obs}, see Figure 3, right, for the exact locations of the evaluation points $(x_1^o, x_2^o) \in \Omega_{\text{obs}}$. Moreover, Figure 3, left, displays a contour plot of a (cubic spline) interpolation of the resulting evacuation times. We observe that, depending on its position, the presence of the obstacle may sensibly improve or deteriorate the evacuation time, which varies between 8.425 and 19.1, thus ranging between about -41% and $+32\%$. Notice also that, when $(x_1^o, x_2^o) = (0.2, 0.2)$, we stop the numerical integration at time $t = 21$, even though the walking domain is not empty yet. The minimum $T_{\text{opt}} = 8.425$ is reached at $(x_1^{\text{opt}}, x_2^{\text{opt}}) = (0, -0.7)$, with the obstacle lying in the corridor traveled by the smallest group, just before the intersection. The solution corresponding to the optimal case is shown in Figure 4. Additionally, Figure 5 provides an insight of the comparison between the reference case and the optimal one, showing also the differences between the evacuation trends of the two populations.

Observe that, according to Corollary 4, the solution $\boldsymbol{r}$ to system (22) linearized at the optimal solution, namely (16), must satisfy (21), i.e.

$$\int_0^{+\infty} \int_\Omega \left(r^1(t, \mathbf{x}) + r^2(t, \mathbf{x}) \right) \mathrm{d}\mathbf{x}\, \mathrm{d}t = 0.$$

To check this, instead of solving (16), which is complicate to implement, here we rely on gradient computation by finite differences. Let us denote by $\boldsymbol{\rho}_{\text{opt}}$ the (numerical) solution to the case with obstacle located in $(x_1^{\text{opt}}, x_2^{\text{opt}})$, thus corresponding to the minimum evacuation time, and by $\boldsymbol{\rho}_h$ the (numerical) solution corresponding to a shift of the obstacle from the optimal position by $h > 0$ in

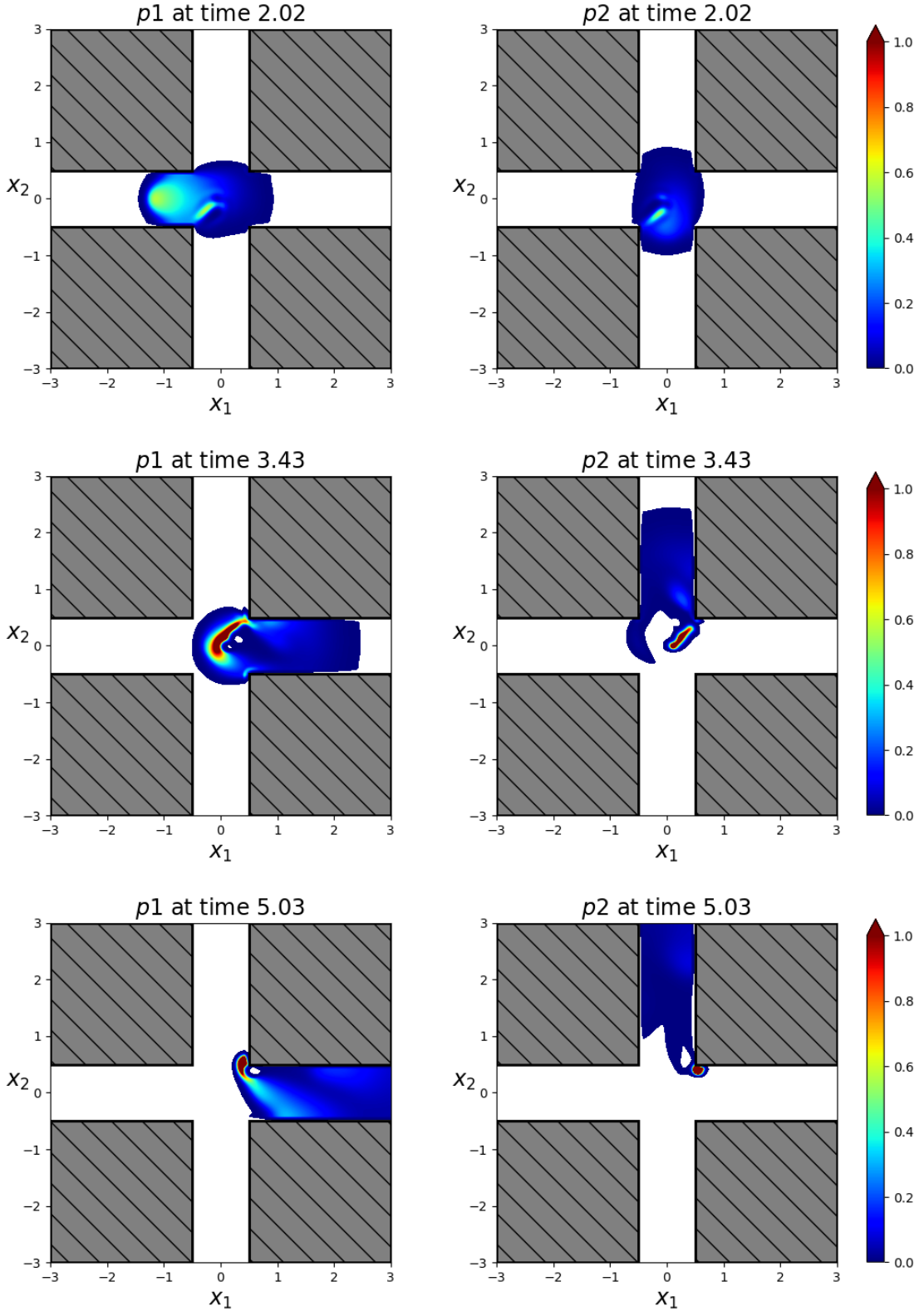

Figure 2: Solution to (22) with no obstacle, i.e. $\Omega_1^c = \emptyset$ at times $t = 2.02$ (top), $t = 3.43$ (middle) and $t = 5.03$ (bottom). Left: ρ^1 (West-East). Right: ρ^2 (South-North).

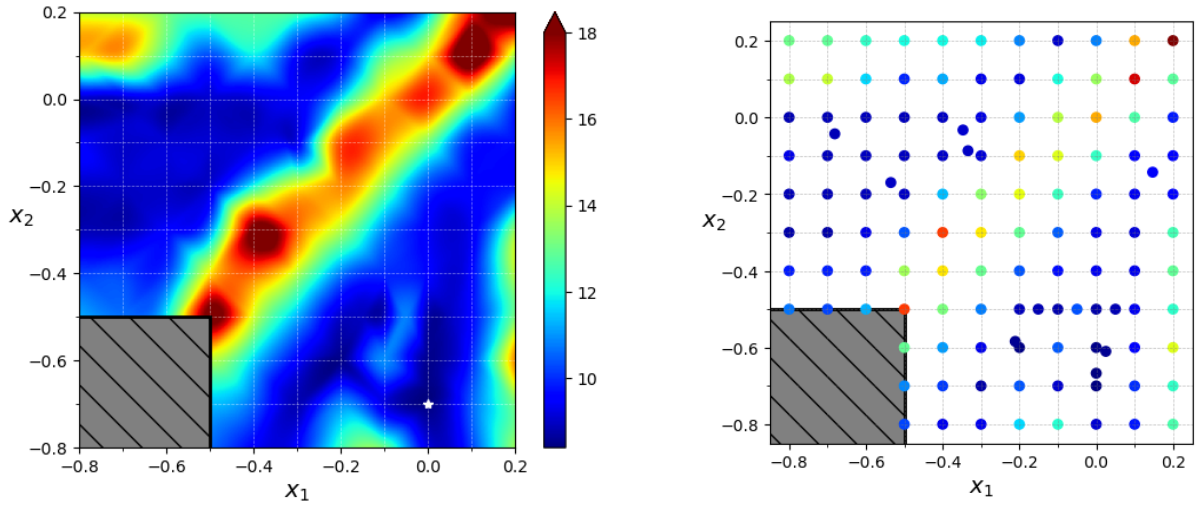

Figure 3: Left: contour plot of the evacuation time as a function of the position of the lower left corner of the obstacle $(x_1^o, x_2^o) \in \Omega_{\text{obs}}$. The picture has been obtained by a (cubic spline) interpolation of the evacuation times computed numerically on the grid displayed on the right. The minimum is $T_{\text{opt}} = 8.425$, reached in $(x_1^{\text{opt}}, x_2^{\text{opt}}) = (0, -0.7)$, see the white star in the left picture.

a given direction $\mathbf{e} = (e_1, e_2)$, thus located at $(x_1^{\text{opt}} + he_1, x_2^{\text{opt}} + he_2)$. Then the quantity

$$q_{\mathbf{e}}^h := \frac{1}{h} \int_0^{+\infty} \int_\Omega \sum_{k=1}^{2} \left(\rho_h^k(t, \mathbf{x}) - \rho_{\text{opt}}^k(t, \mathbf{x}) \right) \mathrm{d}\mathbf{x}\, \mathrm{d}t \approx D_{\mathbf{e}} J(x_1^{\text{opt}}, x_2^{\text{opt}})$$

should have non-negative components close to 0. To check this, we compute $q_{\mathbf{e}}^h$ in the directions $\mathbf{e}_{\pm 1} = (\pm 1, 0)$ and $\mathbf{e}_{\pm 2} = (0, \pm 1)$, shifting the position of the obstacle by $h = 0.1$ in both directions along the Cartesian axes, i.e. computing $\boldsymbol{\rho}_h$ corresponding to the obstacle positions $(x_1^{\text{opt}} \pm h, x_2^{\text{opt}})$ and $(x_1^{\text{opt}}, x_2^{\text{opt}} \pm h)$. This results in:

$$q_{+2}^h = \begin{pmatrix} 0 \\ 0.578 \end{pmatrix}, \qquad q_{-2}^h = \begin{pmatrix} 0 \\ 0.205 \end{pmatrix}, \qquad q_{-1}^h = \begin{pmatrix} 0.883 \\ 0 \end{pmatrix}, \qquad q_{+1}^h = \begin{pmatrix} 1.258 \\ 0 \end{pmatrix},$$

which confirms the optimality of $(x_1^{\text{opt}}, x_2^{\text{opt}})$.

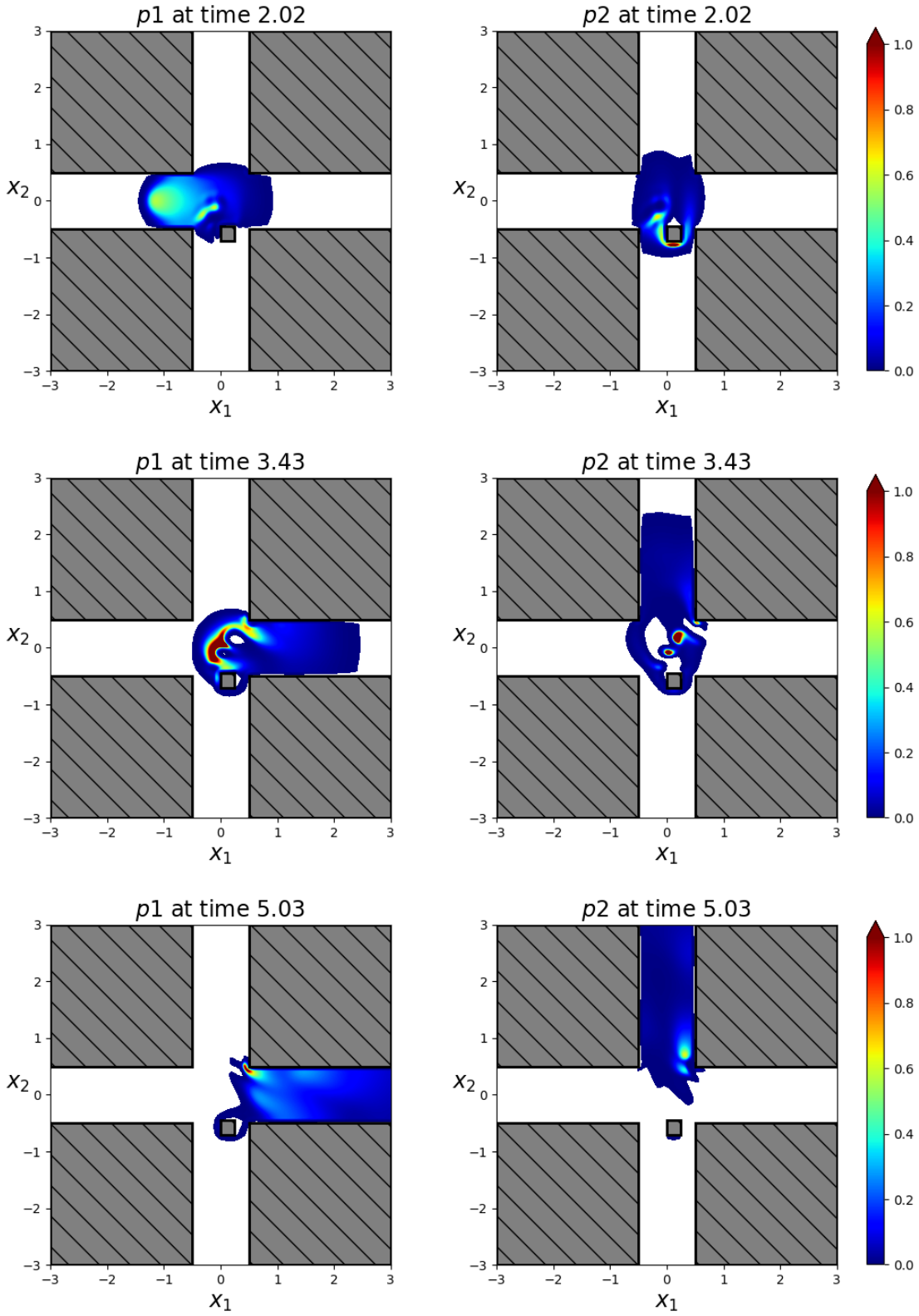

Figure 4: Solution to (22) with the obstacle located in the optimal position, i.e. $\Omega_1^c =]0, 0.25[\times]-0.7, -0.45[$, at times $t = 2.02$ (top), $t = 3.43$ (middle) and $t = 5.03$ (bottom). Left: ρ^1 (West-East). Right: ρ^2 (South-North).

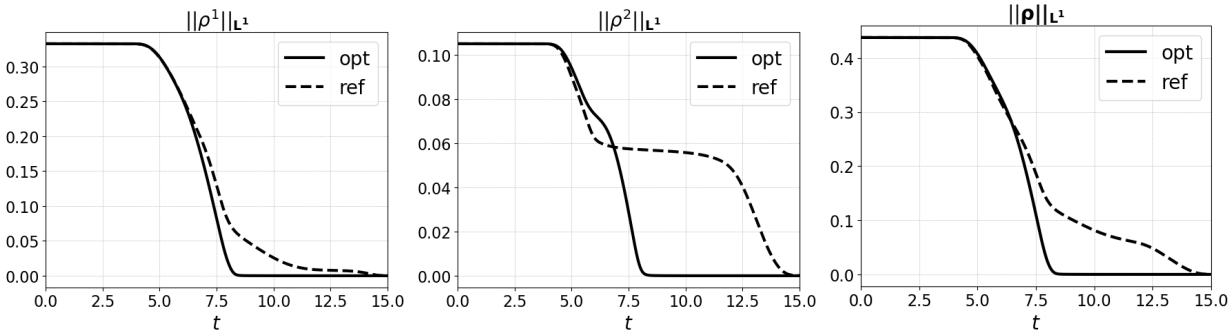

Figure 5: Form left to right: time evolution of mass of the first population ($\left\|\rho^1(t,\cdot)\right\|_{\mathbf{L^1}(\Omega)}$), the second population ($\left\|\rho^2(t,\cdot)\right\|_{\mathbf{L^1}(\Omega)}$) and the total mass ($\left\|\rho^1(t,\cdot)+\rho^2(t,\cdot)\right\|_{\mathbf{L^1}(\Omega)}$) in the reference case without obstacle (dashed line) and in the case of optimal position of the obstacle (continuous line).

5 Conclusions

Leveraging the idea of implementing the presence of obstacles in the nonlocal operator [5, 17], we have proved the $\mathbf{L^1}$ stability of the crowd density distributions of different groups of pedestrians solving (1) with respect to the shape of the walking domain. In turn, this ensures the existence of solutions to optimal control problems depending on the shape of the domain, such as the optimal positions of obstacles to minimize the evacuation time of a crowd from a given facility. In the linear case (14), a differentiability result also provides necessary conditions for optimal solutions.
These results have been illustrated on a particular example of two groups crossing perpendicularly in a cross shaped domain, but can be applied to any other configuration.

The proposed approach can be extended to other nonlocal models dealing with solid boundaries, such as [19], greatly improving the coding and computational costs of solving optimization problems depending on the shape of the physical domain.

Acknowledgments

ER was partially supported by the 2024 INdAM GNAMPA project *Modelling and Analysis through Conservation Laws*. ER acknowledges the PRIN 2022 project *Modeling, Control and Games through Partial Differential Equations* D53D23005620006, funded by the European Union-Next Generation EU.

References

[1] A. Aggarwal, R. M. Colombo, and P. Goatin. Nonlocal systems of conservation laws in several space dimensions. *SIAM J. Numer. Anal.*, 53(2):963–983, 2015.

[2] A. Aggarwal and P. Goatin. Crowd dynamics through non-local conservation laws. *Bull. Braz. Math. Soc. (N.S.)*, 47(1):37–50, 2016.

[3] N. Bellomo and C. Dogbé. On the modelling crowd dynamics from scaling to hyperbolic macroscopic models. *Math. Models Methods Appl. Sci.*, 18:1317–1345, 2008.

[4] S. Blandin and P. Goatin. Well-posedness of a conservation law with non-local flux arising in traffic flow modeling. *Numer. Math.*, 132(2):217–241, 2016.

[5] R. Bürger, P. Goatin, D. Inzunza, and L. M. Villada. A non-local pedestrian flow model accounting for anisotropic interactions and domain boundaries. *Math. Biosci. Eng.*, 17(5):5883–5906, 2020.

[6] F. A. Chiarello, P. Goatin, and E. Rossi. Stability estimates for non-local scalar conservation laws. *Nonlinear Anal. Real World Appl.*, 45:668–687, 2019.

[7] R. M. Colombo, M. Garavello, and M. Lécureux-Mercier. A class of nonlocal models for pedestrian traffic. *Math. Models Methods Appl. Sci.*, 22(4):1150023, 34, 2012.

[8] R. M. Colombo, M. Herty, and M. Mercier. Control of the continuity equation with a non local flow. *ESAIM Control Optim. Calc. Var.*, 17(2):353–379, 2011.

[9] R. M. Colombo and M. Lécureux-Mercier. Nonlocal crowd dynamics models for several populations. *Acta Math. Sci. Ser. B (Engl. Ed.)*, 32(1):177–196, 2012.

[10] R. M. Colombo and M. D. Rosini. Pedestrian flows and nonclassical shocks. *Math. Methods Appl. Sci.*, 28(13):1553–1567, 2008.

[11] R. M. Colombo and E. Rossi. Nonlocal conservation laws in bounded domains. *SIAM J. Math. Anal.*, 50(4):4041–4065, 2018.

[12] R. M. Colombo and E. Rossi. Modelling crowd movements in domains with boundaries. *IMA J. Appl. Math.*, 84(5):833–853, 2019.

[13] G. Crippa and M. Lécureux-Mercier. Existence and uniqueness of measure solutions for a system of continuity equations with non-local flow. *NoDEA Nonlinear Differential Equations Appl.*, 20(3):523–537, 2013.

[14] M. C. Delfour and J.-P. Zolésio. *Shapes and geometries*, volume 22 of *Advances in Design and Control*. Society for Industrial and Applied Mathematics (SIAM), Philadelphia, PA, second edition, 2011. Metrics, analysis, differential calculus, and optimization.

[15] R. Etikyala, S. Göttlich, A. Klar, and S. Tiwari. Particle methods for pedestrian flow models: from microscopic to nonlocal continuum models. *Math. Models Methods Appl. Sci.*, 24(12):2503–2523, 2014.

[16] G. Frank and C. Dorso. Room evacuation in the presence of an obstacle. *Physica A: Statistical Mechanics and its Applications*, 390(11):2135–2145, 2011.

[17] P. Goatin, D. Inzunza, and L. M. Villada. Nonlocal macroscopic models of multi-population pedestrian flows for walking facilities optimization. working paper or preprint, 2023.

[18] P. Goatin, D. Inzunza, and L. M. Villada. Numerical comparison of nonlocal macroscopic models of multi-population pedestrian flows with anisotropic kernel. In C. Parés, M. J. Castro, T. Morales de Luna, and M. L. Muñoz-Ruiz, editors, *Hyperbolic Problems: Theory, Numerics, Applications. Volume II*, pages 371–381, Cham, 2024. Springer Nature Switzerland.

[19] S. Göttlich, S. Hoher, P. Schindler, V. Schleper, and A. Verl. Modeling, simulation and validation of material flow on conveyor belts. *Appl. Math. Model.*, 38:3295–3313, 2014.

[20] D. Helbing, I. J. Farkas, and T. Vicsek. *Crowd Disasters and Simulation of Panic Situations*, pages 330–350. Springer Berlin Heidelberg, Berlin, Heidelberg, 2002.

[21] D. Helbing and P. Molnár. Social force model for pedestrian dynamics. *Phys. Rev. E*, 51:4282–4286, May 1995.

[22] S. P. Hoogendoorn, F. L. van Wageningen-Kessels, W. Daamen, and D. C. Duives. Continuum modelling of pedestrian flows: From microscopic principles to self-organised macroscopic phenomena. *Physica A: Statistical Mechanics and its Applications*, 416:684–694, 2014.

[23] R. L. Hughes. A continuum theory for the flow of pedestrians. *Transpn. Res.–B*, 36(6):507–535, 2002.

[24] R. L. Hughes. The flow of human crowds. In *Annual review of fluid mechanics, Vol. 35*, volume 35 of *Annu. Rev. Fluid Mech.*, pages 169–182. Annual Reviews, Palo Alto, CA, 2003.

[25] Y. Jiang, P. Zhang, S. Wong, and R. Liu. A higher-order macroscopic model for pedestrian flows. *Physica A*, 389(21):4623 – 4635, 2010.

[26] K. H. Karlsen and N. H. Risebro. On the uniqueness and stability of entropy solutions of nonlinear degenerate parabolic equations with rough coefficients. *Discrete Contin. Dyn. Syst.*, 9(5):1081–1104, 2003.

[27] A. Keimer, L. Pflug, and M. Spinola. Existence, uniqueness and regularity of multi-dimensional nonlocal balance laws with damping. *J. Math. Anal. Appl.*, 466(1):18–55, 2018.

[28] S. N. Kružkov. First order quasilinear equations with several independent variables. *Mat. Sb. (N.S.)*, 81 (123):228–255, 1970.

[29] N. Maltugueva and N. Pogodaev. Modeling of crowds in regions with moving obstacles. *Discrete Contin. Dyn. Syst.*, 41(11):5009–5036, 2021.

[30] B. Maury, A. Roudneff-Chupin, and F. Santambrogio. A macroscopic crowd motion model of gradient flow type. *Math. Models Methods Appl. Sci.*, 20:1787–1821, 2009.

[31] B. Piccoli and A. Tosin. Pedestrian flows in bounded domains with obstacles. *Contin. Mech. Thermodyn.*, 21(2):85–107, 2009.

[32] E. Rossi, J. Weißen, P. Goatin, and S. Göttlich. Well-posedness of a non-local model for material flow on conveyor belts. *ESAIM Math. Model. Numer. Anal.*, 54(2):679–704, 2020.

[33] M. Twarogowska, P. Goatin, and R. Duvigneau. Macroscopic modeling and simulations of room evacuation. *Appl. Math. Model.*, 38(24):5781–5795, 2014.